Supplementary Information: Methods/Tables/Figures

Prevention of radiotherapy-induced pro-tumorigenic microenvironment by SFK inhibitors

Yong June Choi[1], Myung Jun Kim[1], Young Joo Lee[1], Munkyung Choi[1], Wan Seob Shim[1], Miso Park[2], Yong-Chul Kim[3] and Keon Wook Kang[1,*]

[1]College of Pharmacy, Research Institute of Pharmaceutical Sciences and Natural Products Research Institute, Seoul National University, Seoul 08826, Republic of Korea. [2]Department of Pharmacy, Kangwon National University, Chuncheon 24341, Republic of Korea. [3]School of Life Sciences, Gwangju Institute of Science and Technology, Gwangju 61005, Republic of Korea.

Corresponding Author: Keon Wook Kang, Ph.D. E-mail: kwkang@snu.ac.kr

Supplementary Materials and Methods

Immunohistochemistry (IHC)

For IHC, the lung tissues were dissected from sacrificed mice. Paraffin blocks were prepared and subsequent staining was conducted using specific F4/80 antibody or TGF-beta 1 antibody. Stained slides were photographed using a Vectra instrument (PerkinElmer). The used IHC antibodies are listed in **Table S3**.

Cytokine array

The mouse chest underwent a single irradiation with 22 Gy, and the mouse lungs were dissected three days later. Isolated lung tissues were processed according to the cytokine array manufacturer's manual (#AAM-BLM-1-2, Raybiotech, Norcross, GA, USA). Briefly, the isolated lungs were lysed using the provided lysis buffer, and supernatant was quantified and biotinylated. The biotinylated sample underwent a reaction with the membrane, and following washing, HRP-conjugated streptavidin was applied. Membranes were visualized and detected by LAS-3000 mini (Fujifilm).

Macrophage cell viability assessment

Macrophages were seeded in 96-well plates (2×10^4 cells/well) and were treated with NXP900. After 24 h incubation, 10 μL WST-8 solution (#CM-VA1000, Precaregene, Anyang, South Korea) were added and incubated for additional 4 h in the dark. The absorbance at 450 nm was measured using a multi-mode microplate reader (SpectraMax iD3, Molecular Devices, San Jose, CA, USA) to calculate the number of viable cells.

M2 differentiation of macrophages

The mouse bone marrow cells were seeded into a petri dish, and treated with 30 ng/ml

macrophage-colony stimulating factor (M-CSF) for 6 days to induce macrophage differentiation. Differentiated macrophages were treated with TGF-β 5 ng/ml or IL-4 20 ng/ml for 24 h for further M2 differentiation.

In vitro proliferation and migration assays

For the proliferation assay, cancer cells were seeded in 96-well plate (2 x 10^3 cells/well), and after the drug treatment, cell confluence was scanned and analyzed by the IncuCyte Zoom device (EssenBioscience). For the transwell migration assay, cancer cells (3,000 cells/upper well) were seeded in the IncuCyte Clearview 96-well plate (#4582, Sartorius). To create a gradient of chemoattractant, 1% FBS was added to the upper well, while 15% FBS was added to the lower well. Drugs were added to both the upper and lower wells at the indicated concentrations. The number of cells above and below was scanned and analyzed by the IncuCyte Zoom device (EssenBioscience).

Statistical analysis

Statistical significance was determined using GraphPad Prism 7.0. The significance between experimental groups were analyzed using either one-way ANOVA followed by Tukey's test or an unpaired two-tailed Student t-test. *P* values less than 0.05 were considered as significant differences. *P* value presented in this study follows the NEJM style; *$p < 0.05$, **$p < 0.01$, ***$p < 0.001$.

Supplementary Tables

Table S1. The used cell lines and their respective culture methods.

Cell line	Culture Medium
4T1	RPMI-1640 medium + 10% FBS + 1% P/S
4T1-luc	RPMI-1640 medium + 10% FBS + 1% P/S
B16F10	High glucose DMEM medium + 10% FBS + 1% P/S
B16F10-luc	High glucose DMEM medium + 10% FBS + 1% P/S
THP1	RPMI-1640 medium + 10% FBS + 1% P/S
MRC5	RPMI-1640 medium + 10% FBS + 1% P/S
BEAS2B	High glucose DMEM medium + 10% FBS + 1% P/S
LX2	High glucose DMEM medium + 10% FBS + 1% P/S

DMEM: Dulbecco's modified Eagle's medium

FBS: Fetal bovine serum, Thermo Fisher Scientific, Waltham, MA, USA

P/S: penicillin/streptomycin, Hyclone, Logan, UT, USA

Table S2. The specific primer sequences employed in study.

Name	Forward (5'-3')	Reverse (5'-3')
Timp1	CTTGGTTCCCTGGCGTACTC	ACCTGATCCGTCCACAAACAG
Acta2	GGCTCTGGGCTCTGTAAGG	CTCTTGCTCTGGGCTTCATC
Col1a1	GCCCGAACCCCAAGGAAAAGAAGC	CTGGGAGGCCTCGGTGGACATTAG
Tgf-beta1	TCGACATGGAGCTGGTGAAA	GGGACTGGCGAGCCTTAGTT
Src	GTTGCTTCGGAGAGGTGTGGAT	CACCAGTTTCTCGTGCCTCAGT
Yes1	GGTCTGGCAAAAGATGCTTGGG	GGCATCATTGTACCTGGCTTTAG
18s rRNA	AGGATCCATTGGAGGGCAAGT	TCCAACTACGAGCTTTTTAACTGCA

Table S3. The used antibodies.

Antibodies for western blotting

Name	Company	Cat No.
COX-2	Abcam (Cambridge, UK)	Ab15191
Arginase-1	Santa Cruz Biotechnology (Dallas, TX, USA)	sc-271430
YAP		sc-376830
GAPDH	Merck Millipore (Burlington, MA, USA)	CB1001
Mouse YES1	Proteintech (Rosemont, IL, USA)	20243-1-AP
Phospho-SFK	Cell Signaling Technology (Danvers, MA, USA)	2101s
SRC		2108s
YES1		3201s
Phospho-Smad2		3101s
Phospho-p70S6K		9234s
Phospho-AKT		9271s
Phospho-MEK		9154s
Phospho-ERK		9101s
Phospho-YAP		4911s
Phospho-Cortactin		4569s
SMAD2		5339s
p70S6K		9202s
AKT		9272s
MEK		8727s
ERK		9102s
Cortactin		3502s
HRP-linked anti-rabbit IgG		7074s

HRP-linked anti-mouse IgG		7076s
α-SMA	Sigma-Aldrich (St. Louis, MO, USA)	A5228
PAI-1	BD Biosciences (Franklin Lakes, NJ, USA)	612024
E-cadherin		610181
N-cadherin		610920

Antibodies for flow cytometry

Name	Company	Cat No.
PE anti-mouse CD45	Biolegend (San Diego, CA, USA)	103105
APC anti-mouse F4/80		123115
FITC anti-mouse Ly6G		127605
APC/Cy7 anti-mouse CD19		115530
APC anti-mouse CD8		100711
FITC anti-mouse CD4		100509
APC/Cy7 anti-mouse CD11c		117324
FITC anti-mouse CD206		141703
APC/Cy7 anti-mouse CD86		105029
PE/Cy7 anti-mouse CD64		139313
PE/Cy5 anti-mouse CD11b		101209
APC anti-mouse SiglecF		155507

Antibodies for in vivo neutralization

Name	Company	Cat No.
InVivoMAb anti-mouse F4/80	Bio X Cell (Lebanon, NH, USA)	BE0206
InVivoMAb anti-mouse PD-1		BE0146

Antibodies for IHC

Name	Company	Cat No.
F4/80	Cell Signaling Technology (Danvers, MA, USA)	70076s
TGF-beta 1	Sigma-Aldrich (St. Louis, MO, USA)	SAB4502954

Supplementary Figures

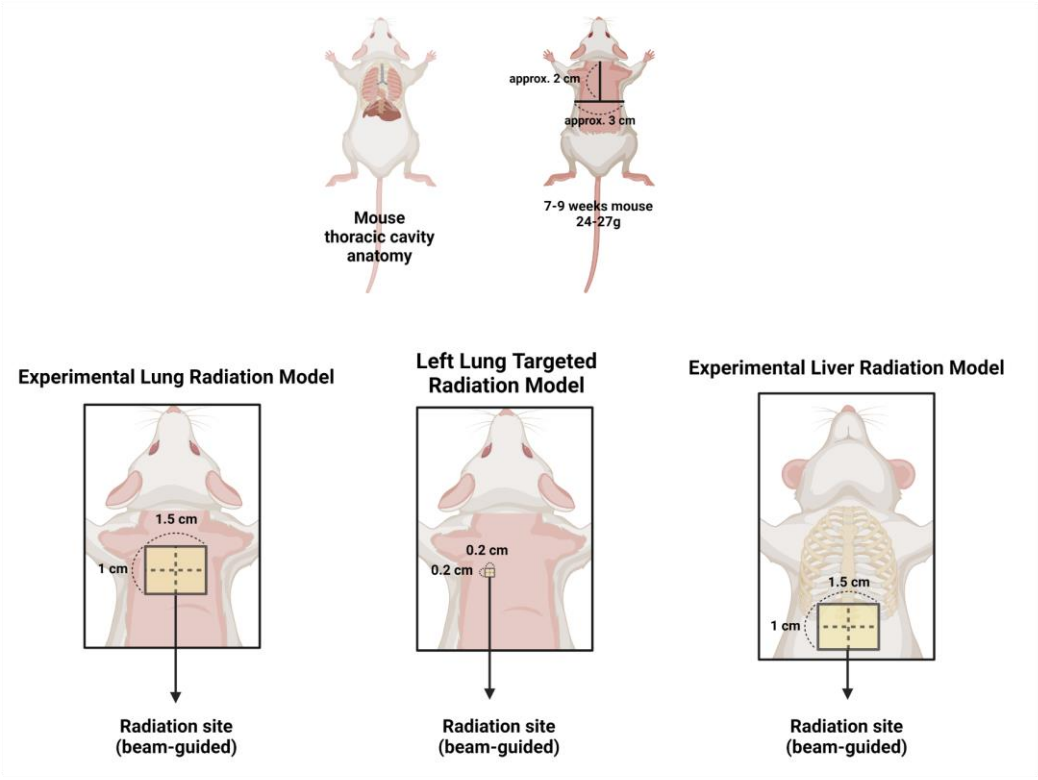

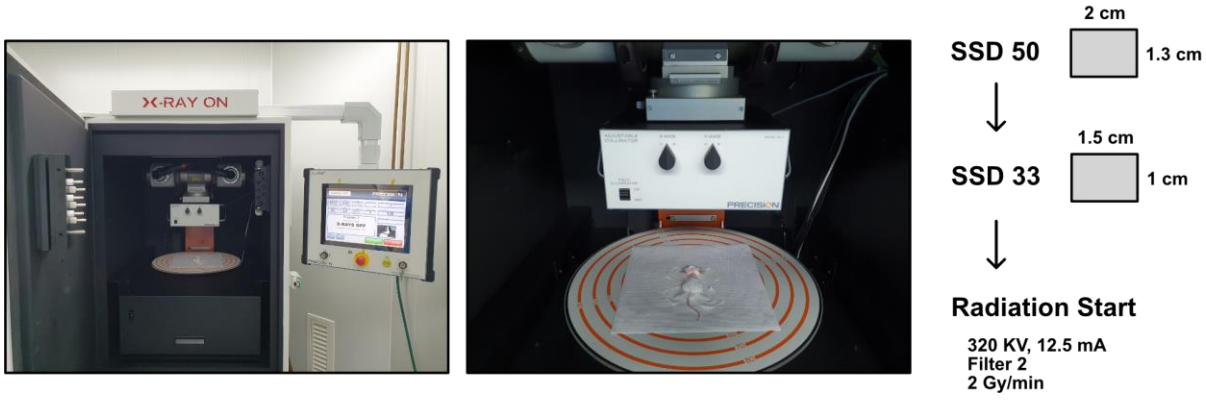

Figure S1. Experimental mouse radiotherapy model

Schematic illustration of experimental mouse radiotherapy model. For the experimental implementation of lung radiotherapy, radiation was delivered to a 1.5 cm×1 cm area on the dorsal of the thoracic cavity (left). To mimic stereotactic body radiotherapy, radiation was delivered to a 0.2 cm×0.2 cm area on the dorsal of the left thoracic cavity (middle). For the experimental implementation of liver radiotherapy, radiation was delivered to a 1.5 cm×1 cm

area on the abdomen (right). The irradiation procedures were conducted using the X-RAD 320 (Precision) equipped with a Dynamic Collimator (Precision) and an F2 filter.

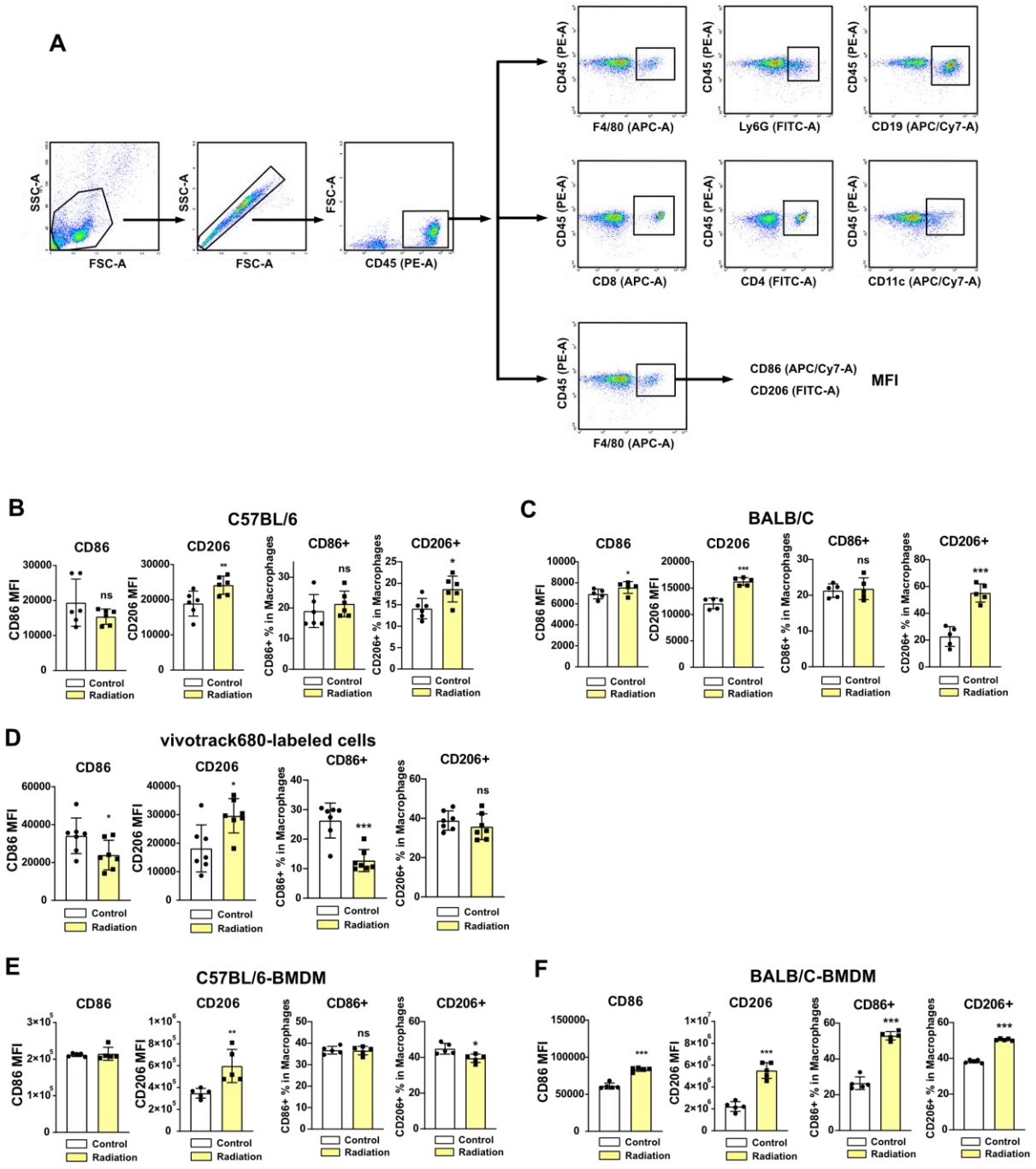

141

142

143 **Figure S2. Gating strategies and individual values of M1, M2 markers**

144 (**A**) Gating strategy for Figure 2 and 8. The used flow cytometry antibodies are listed in Table

145 S3. (**B-F**) Percentage of M1 and M2 macrophages and individual values of CD86 and CD206

146 MFI about Figure 2C, D, F, and I, respectively. All data were presented as mean ± SD.

147 Statistical significance of the differences was determined by two-tailed Student t-test.

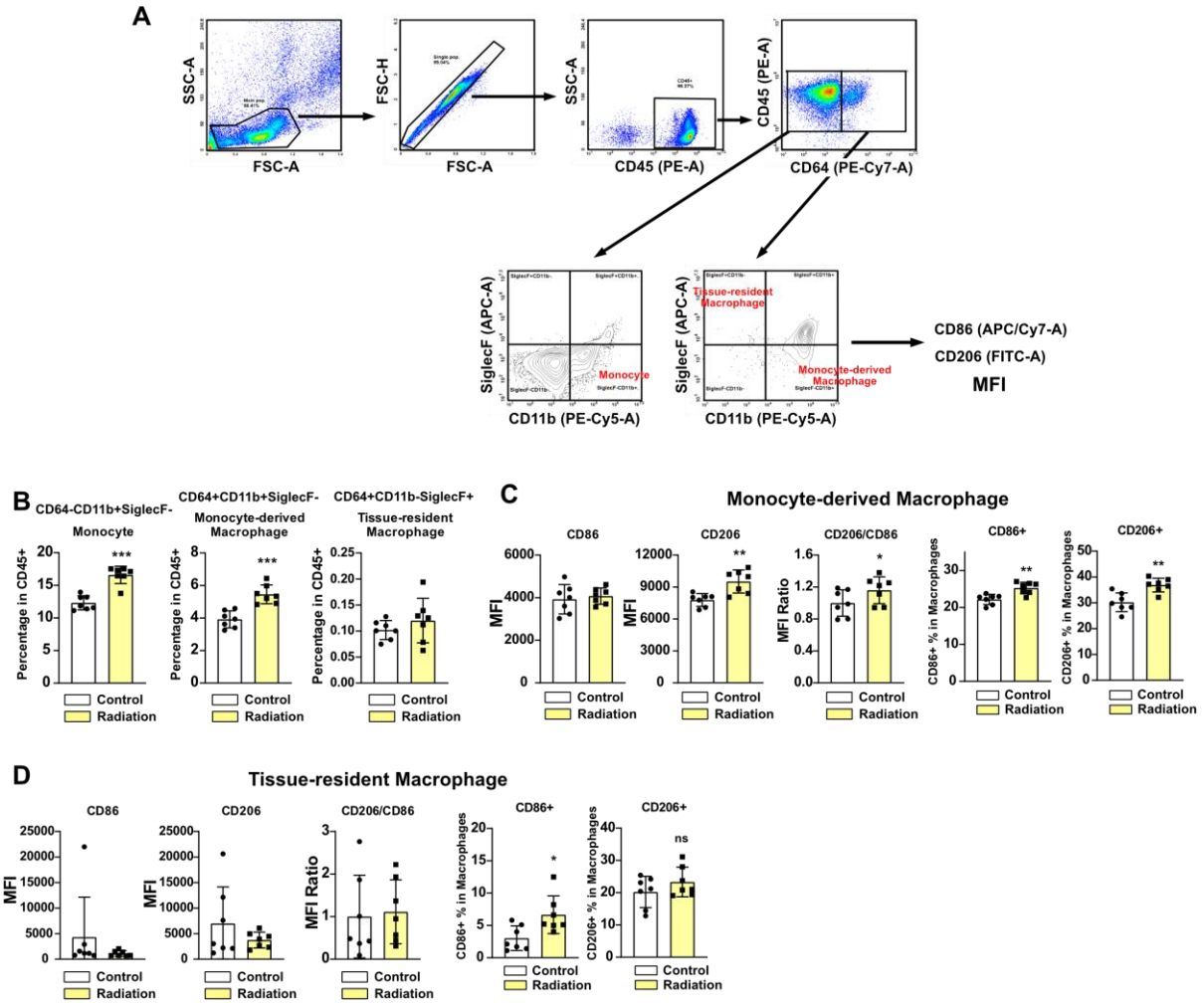

Figure S3. Radiation-induced changes of monocyte-derived macrophages and tissue-resident macrophages in mouse lung tissues

Changes in immune cells infiltration in lung tissues. Lung tissues were collected 2 weeks after radiation (22 Gy×2). *n* = 6/group. (**A**) Gating strategy in flow cytometry. The used flow cytometry antibodies are listed in Table S3. (**B**) Percentage of monocytes (CD45+CD64-CD11b+SiglecF-), monocyte-derived macrophages (CD45+CD64+CD11b+SiglecF-), and tissue-resident macrophages (CD45+CD64+CD11b-SiglecF+) after radiation. (**C**) Radiation-induced M2 differentiation of monocyte-derived macrophages. (**D**) Radiation-induced M2 differentiation of tissue-resident macrophages. All data were presented as mean ± SD. Statistical significance of the differences was determined by two-tailed Student t-test.

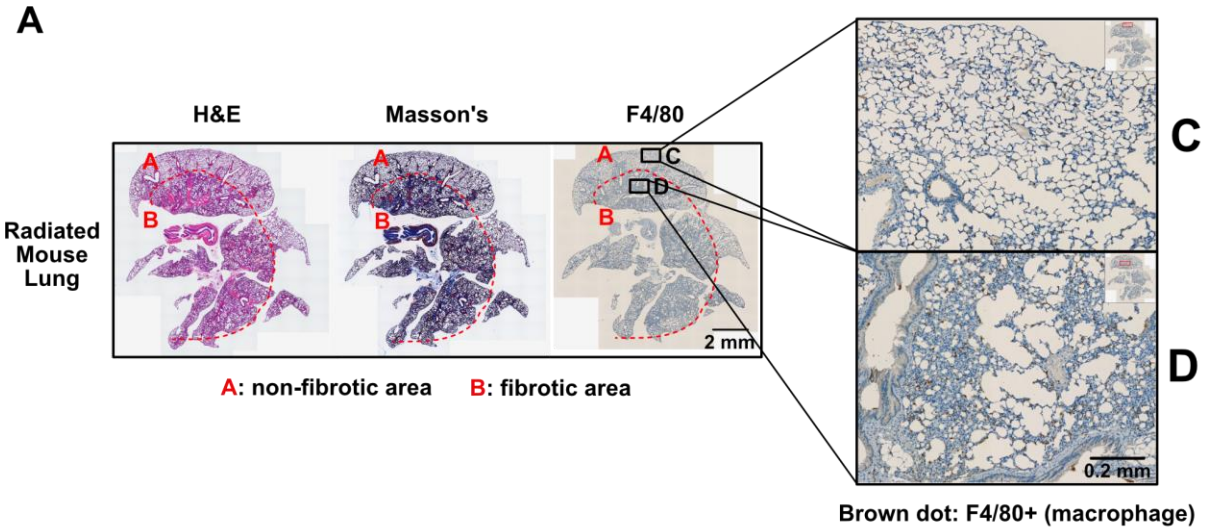

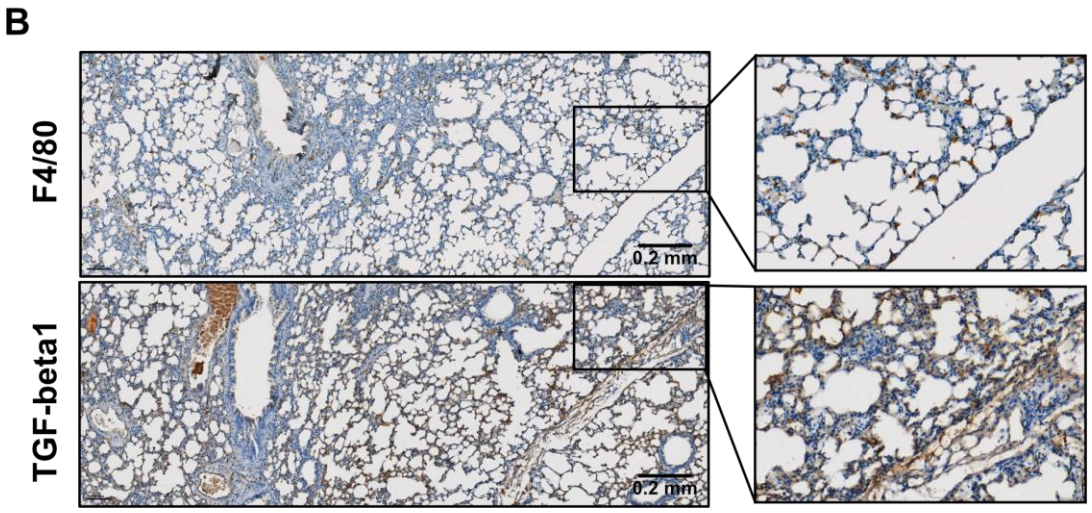

Figure S4. F4/80 and TGF-β1 immunohistochemistry staining at the irradiated site

(**A**) Comparison of F4/80+ macrophage infiltration into irradiated and non-irradiated sites. (**B**) Co-localization of F4/80+ macrophages and TGF-β1. The used IHC antibody is listed in Table S3.

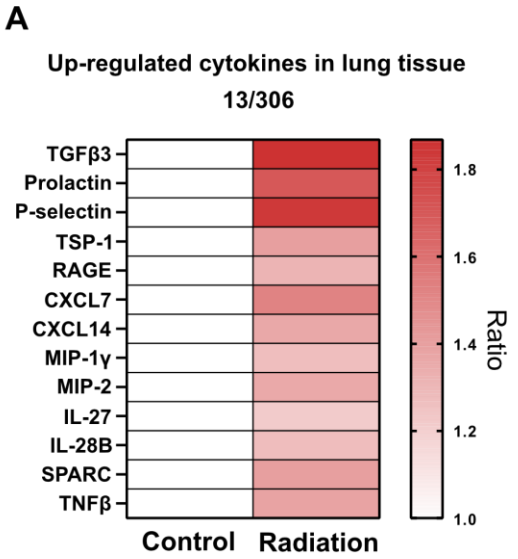

Figure S5. Identification of other cytokines increased in irradiated lung tissue

(**A**) Increased cytokines in irradiated lung tissues were represented. The mouse chest underwent a single irradiation with 22 Gy, and the mouse lungs were dissected three days later. Isolated lung tissues were processed according to the cytokine array manufacturer's manual.

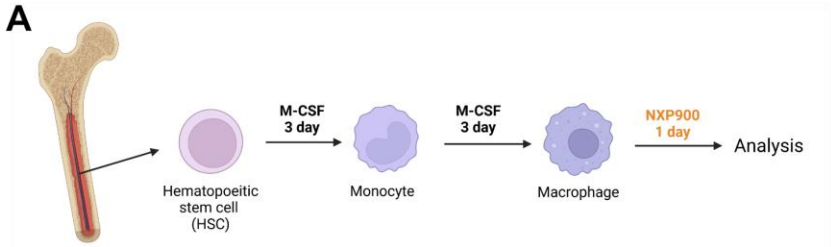
A
M-CSF
3 day
M-CSF
3 day
NXP900
1 day
Analysis
Hematopoeitic
stem cell
(HSC)
Monocyte
Macrophage

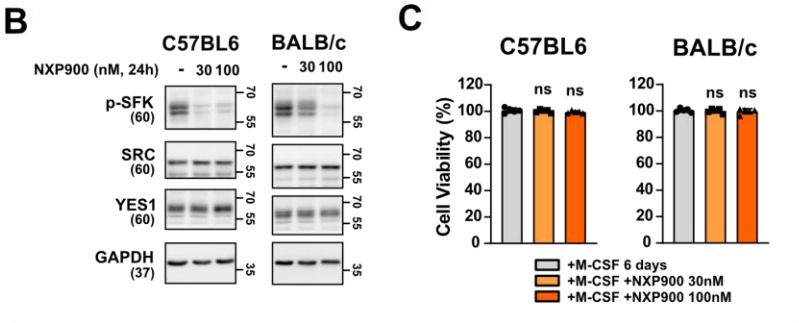
B
C57BL6
BALB/c
NXP900 (nM, 24h)
- 30 100
p-SFK
(60)
SRC
(60)
YES1
(60)
GAPDH
(37)
C
C57BL6
BALB/c
Cell Viability (%)
ns
+M-CSF 6 days
+M-CSF +NXP900 30nM
+M-CSF +NXP900 100nM
D
C57BL6
CD206/CD86
BALB/c
CD206/CD86
MFI Ratio
ns
+M-CSF 6 days
+M-CSF +NXP900 30nM
+M-CSF +NXP900 100nM

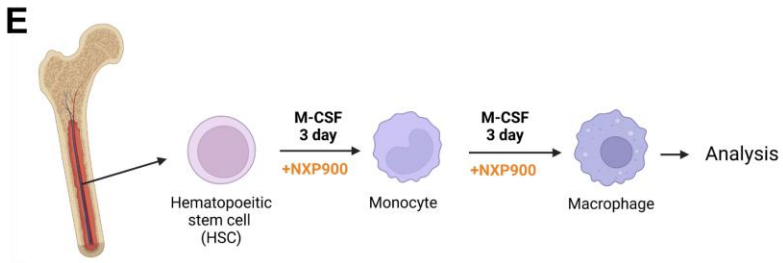
E
M-CSF
3 day
+NXP900
M-CSF
3 day
+NXP900
Analysis
Hematopoeitic
stem cell
(HSC)
Monocyte
Macrophage

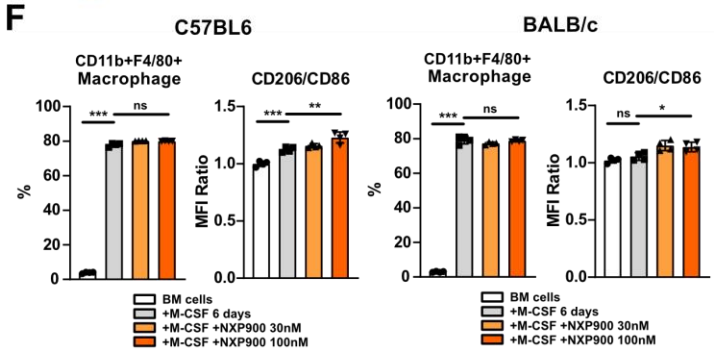
F
C57BL6
BALB/c
CD11b+F4/80+
Macrophage
CD206/CD86
%
MFI Ratio
***
**
*
ns
BM cells
+M-CSF 6 days
+M-CSF +NXP900 30nM
+M-CSF +NXP900 100nM

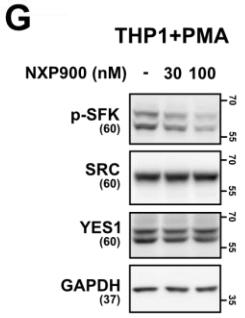
G
THP1+PMA
NXP900 (nM) - 30 100
p-SFK
(60)
SRC
(60)
YES1
(60)
GAPDH
(37)

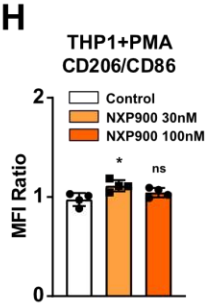
H
THP1+PMA
CD206/CD86
Control
NXP900 30nM
NXP900 100nM
MFI Ratio
*
ns

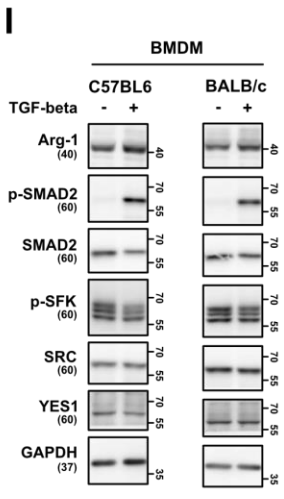
I
BMDM
C57BL6
BALB/c
TGF-beta
- +
Arg-1
(40)
p-SMAD2
(60)
SMAD2
(60)
p-SFK
(60)
SRC
(60)
YES1
(60)
GAPDH
(37)
TGF-beta 5 ng/ml, 24h

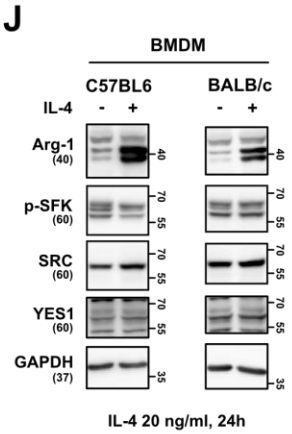
J
BMDM
C57BL6
BALB/c
IL-4
- +
Arg-1
(40)
p-SFK
(60)
SRC
(60)
YES1
(60)
GAPDH
(37)
IL-4 20 ng/ml, 24h

Figure S6. Effect of SFK-targeted inhibitor on macrophage

(**A**) Schematic illustration of the experiment for Figure B-D. (**B**) Confirmation of SFK activity blockade in macrophages following NXP900 treatment. (**C**) Cell viability of macrophages treated with NXP900. (**D**) Effects of NXP900 on differentiated macrophages. (**E**) Schematic illustration of the experiment for Figure F. (**F**) Effects of NXP900 on differentiating macrophages. (**G, H**) Effects of NXP900 on THP1 human macrophages. (**I**) Confirmation of SFK activity during M2 differentiation induced by TGF-β treatment. (**J**) Confirmation of SFK activity during M2 differentiation induced by IL-4 treatment. All data were presented as mean ± SD. Statistical significance of the differences was determined by two-tailed Student t-test or one-way ANOVA followed by the Tukey's test. All western blot analyses in this study were repeated three times independently.

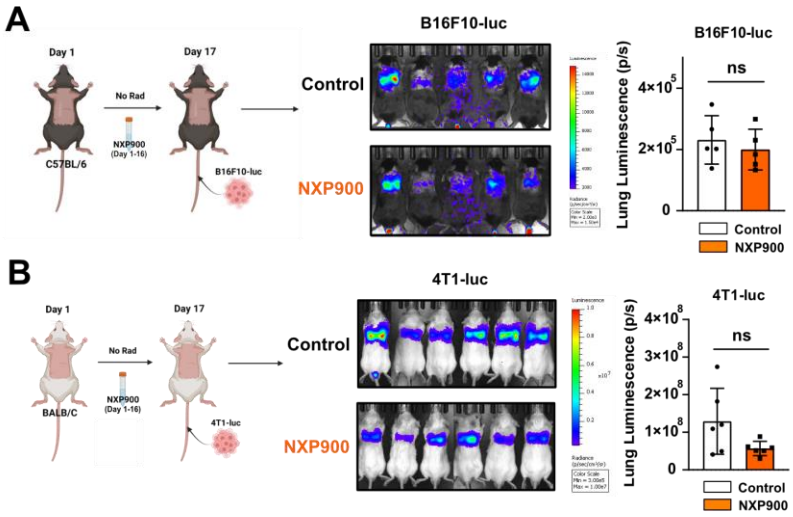

Figure S7. Inhibition of lung engraftment by residual drug

(**A, B**) NXP900 (60 mg/kg, daily, PO) was administered from day 1 to 16. One day after stopping the drug, the cancer cells were injected into the tail vein. *n* = 5 or 6/group. All data were presented as mean ± SD. Statistical significance of the differences was determined by two-tailed Student t-test

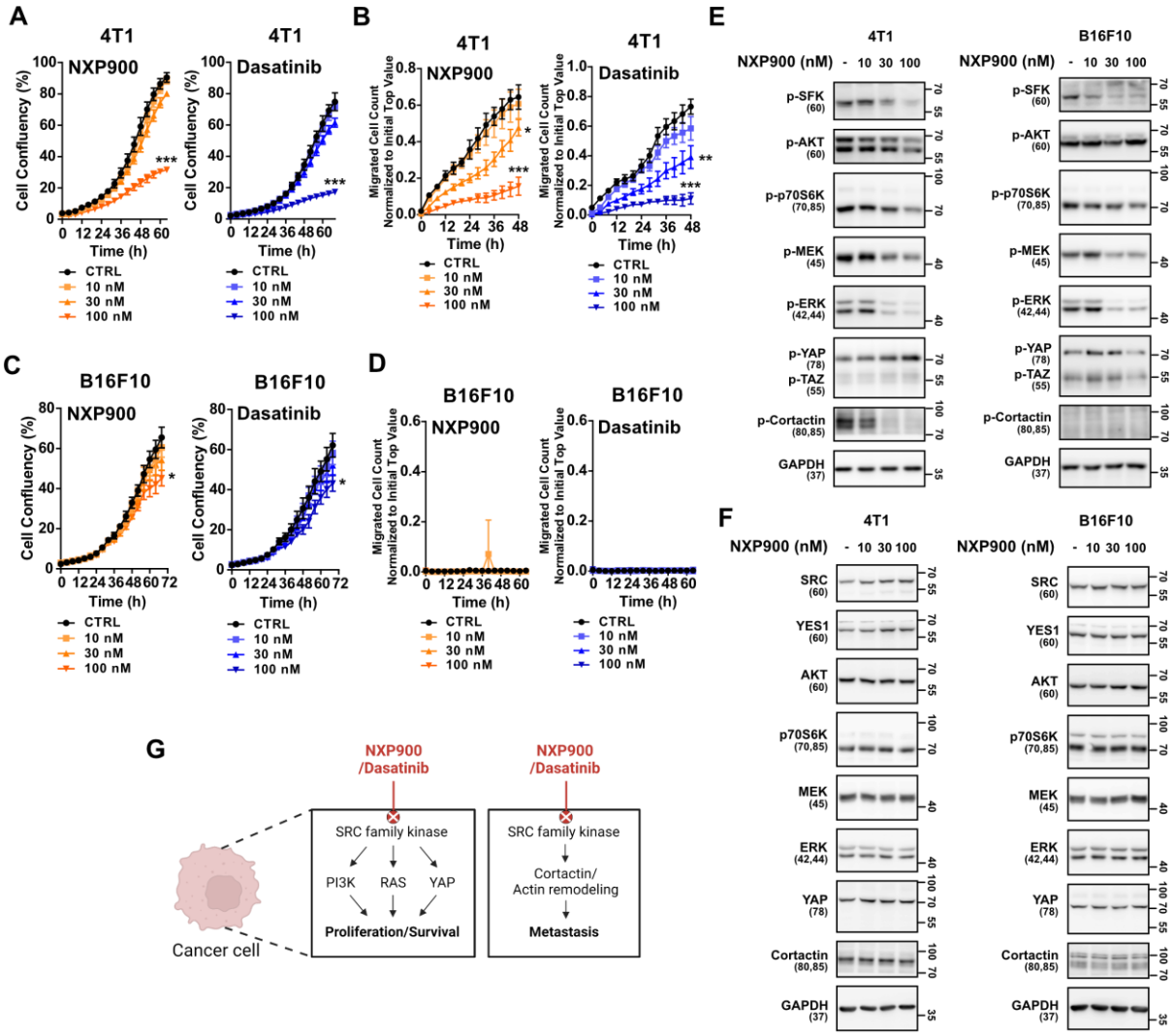

Figure S8. Direct effect of SFK-targeted inhibitors on cancer cells

(**A**) Anti-proliferative activities of SFK-targeted inhibitors in 4T1 mouse breast cancer cells. (**B**) Anti-migratory activities of SFK-targeted inhibitors in 4T1 cells. (**C**) Anti-proliferative activities of SFK-targeted inhibitors in B16F10 mouse melanoma cells. (**D**) Anti-migratory activities of SFK-inhibitors in B16F10 cells. (**E, F**) Inhibition of SFKs downstream pathways by SFK-targeted inhibitors in mouse cancer cells. (**G**) Schematic illustration representing this figure. All data were presented as mean ± SD. Statistical significance of the differences was determined by one-way ANOVA followed by the Tukey's test. All western blot analyses in this study were repeated three times independently.

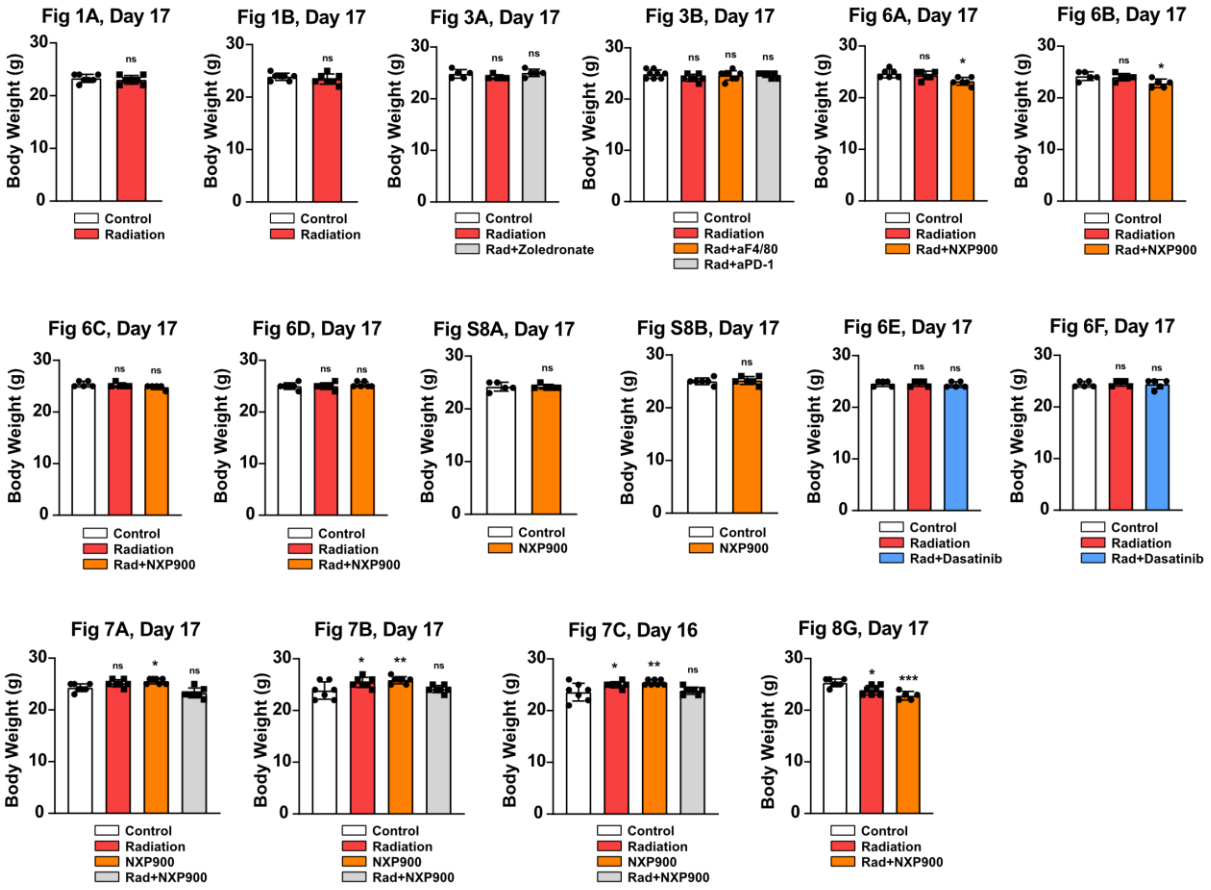

233

234

235 **Figure S9. Body weight changes in animal experiments**

236 In all animal experiments, body weight changes are presented. The corresponding figure
237 number is entered for each graph. All data were presented as mean (SD). Statistical significance
238 of the differences was determined by two-tailed Student t-test or one-way ANOVA followed
239 by the Tukey's test.

240

241

242

243

Figure 1D

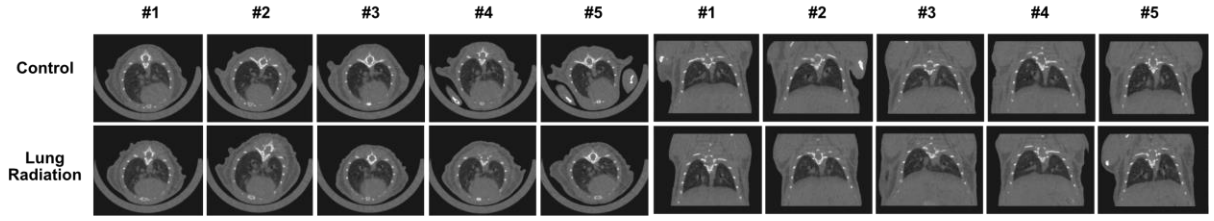

Figure 1F

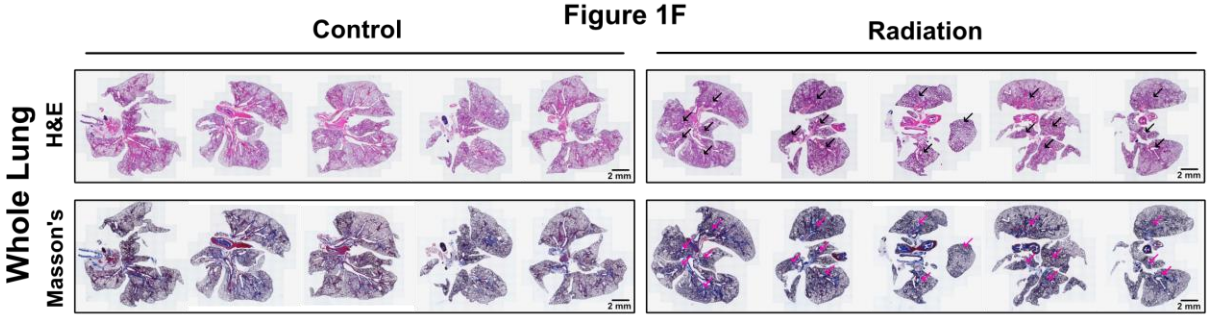

Figure 6G

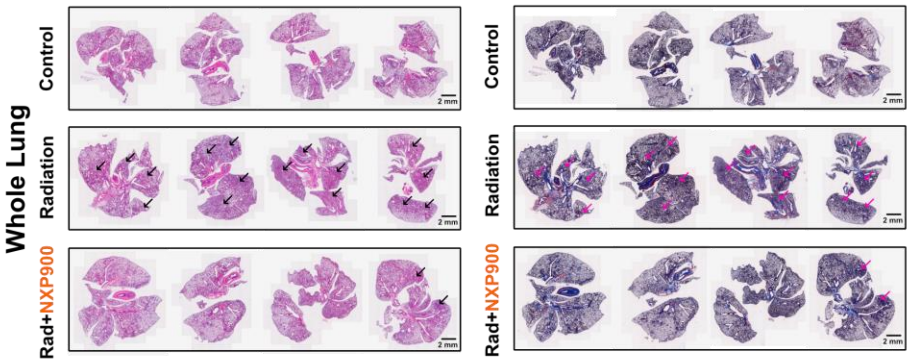

Figure 9B

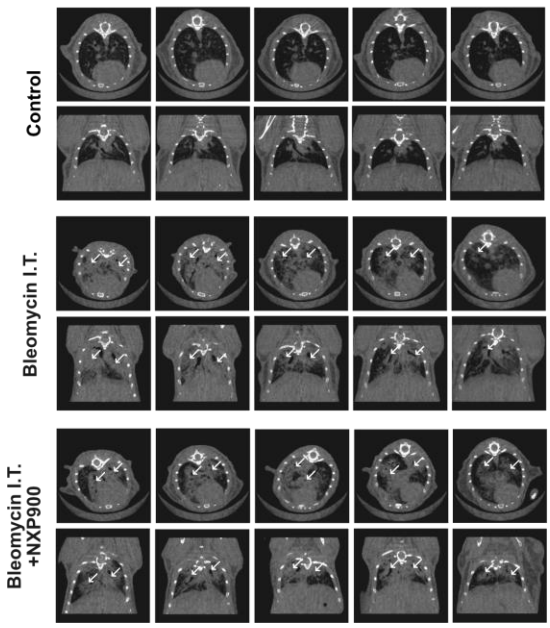

Figure 9E

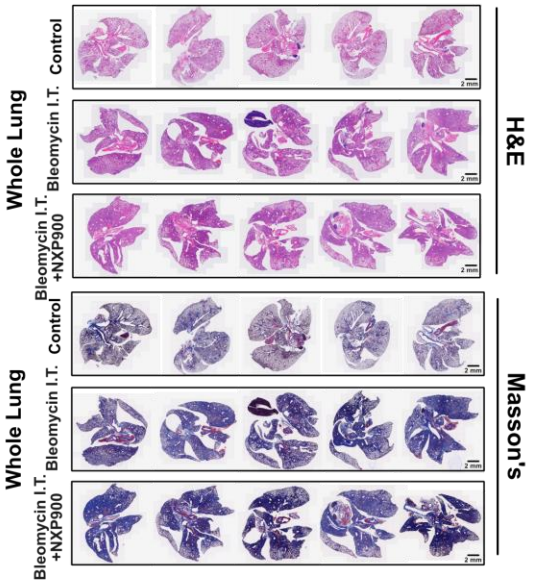

244

245

Figure S10. Individual images of tissue staining and micro-CT from all animal experiments

Individual images of tissue staining and micro-CT from all animal experiments are presented. The corresponding figure number is indicated for each image. Arrows in each image highlight areas of alveolar collapse (H&E staining) and collagen deposition (Masson's trichrome staining).

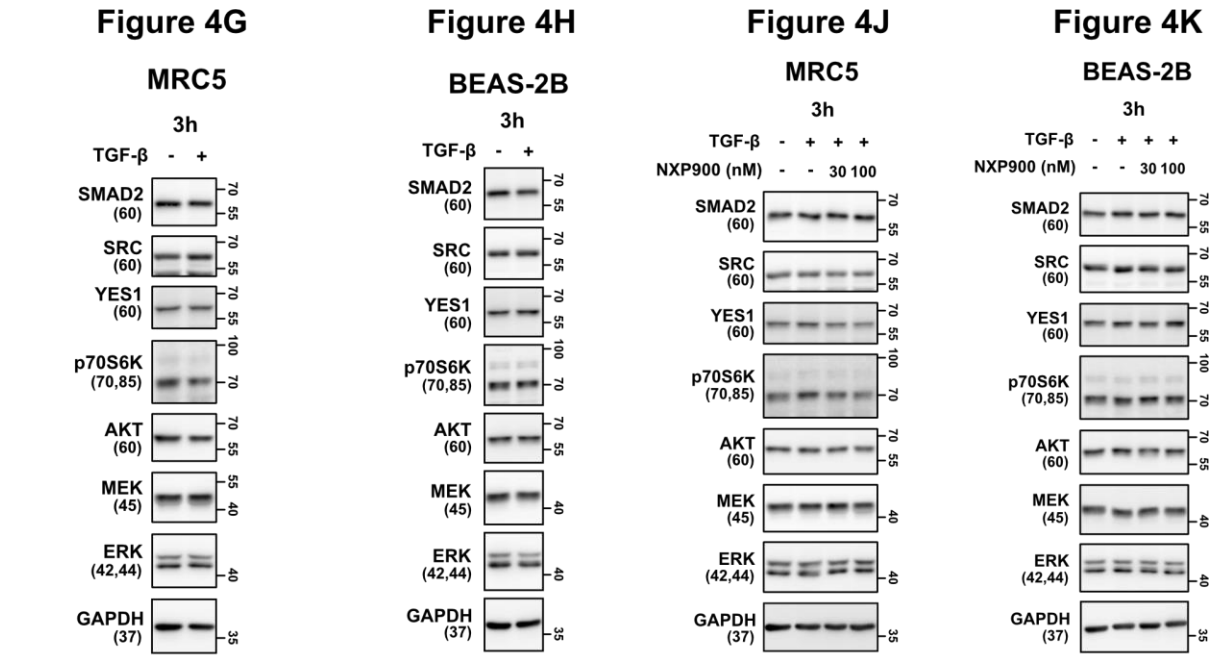

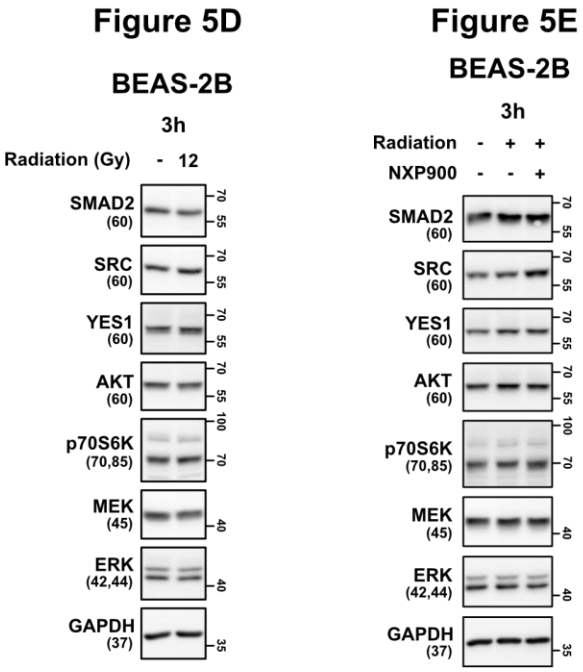

265

266 **Figure S11. Total protein levels for Figure 4 and 5**

267 Total protein levels are presented for Figure 4 and 5, with the corresponding figure numbers
268 indicated for each graph. All western blot analyses in this study were performed independently
269 in triplicate.